Geomechanics and Engineering, *Vol. 22, No. 5 (2020) 375-384*
DOI: https://doi.org/10.12989/gae.2020.22.5.375

Analysis of permeability in rock fracture with effective stress at deep depth

Hangbok Lee[1], Tae-Min Oh*[2] and Chan Park[1]

[1]*Center for Deep Subsurface Research, Korea Institute of Geoscience and Mineral Resources, Daejeon 34132, Republic of Korea*
[2]*Department of Civil and Environmental Engineering, Pusan National University, Busan 46241, Republic of Korea*

(Received July 25, 2019, Revised July 7, 2020, Accepted July 16, 2020)

Abstract. In this study, the application of conventional cubic law to a deep depth condition was experimentally evaluated. Moreover, a modified equation for estimating the rock permeability at a deep depth was suggested using precise hydraulic tests and an effect analysis according to the vertical stress, pore water pressure and fracture roughness. The experimental apparatus which enabled the generation of high pore water pressure (< 10 MPa) and vertical stress (< 20 MPa) was manufactured, and the surface roughness of a cylindrical rock sample was quantitatively analyzed by means of 3D (three-dimensional) laser scanning. Experimental data of the injected pore water pressure and outflow rate obtained through the hydraulic test were applied to the cubic law equation, which was used to estimate the permeability of rock fracture. The rock permeability was estimated under various pressure (vertical stress and pore water pressure) and geometry (roughness) conditions. Finally, an empirical formula was proposed by considering nonlinear flow behavior; the formula can be applied to evaluations of changes of rock permeability levels in deep underground facility such as nuclear waste disposal repository with high vertical stress and pore water pressure levels.

Keywords: deep depth; rock permeability; high vertical stress; high pore water pressure; roughness; nonlinear flow; underground facility; nuclear waste disposal repository

1. Introduction

Nuclear waste includes nuclides which represent a high risk for the environment and for humans. Thus, many countries have been constructing the nuclear waste disposal sites at deep depths of, for instance, 500 m for the long-term isolation of nuclear waste (Ji *et al.* 2012). These deep disposal facilities are mostly located in rock aquifers saturated with groundwater. Therefore, if radioactive contaminants are released from the repository, they are likely to move along the groundwater and be exposed to the biosphere of the surface. In this regard, it is crucial to characterize the surrounding groundwater flow system when designing an underground structure such as radioactive waste repository site or deep tunnel (Wang *et al.* 2017, Kim *et al.* 2018, Deng *et al.* 2019). Generally, because groundwater mainly flows through rock fractures in crystalline rocks, an accurate understanding of the permeability characteristics of rock fractures is most important (Lee *et al.* 2017). Specifically, the permeability characteristics of rock fractures can be affected by high vertical stress (e.g., 20 MPa) and high pore water pressure (e.g., 10 MPa), because nuclear disposal sites are typically located at deep depths up to 500 m.

The permeability of rock fractures can change due to stress variations near fractured rock caused by the formation of underground spaces or heat originating from radioactive waste (Nguyen and Jing 2008, Rutqvist *et al.* 2008, Najari and Selvadurai 2014, Saberhosseini *et al.* 2014). Many researchers have investigated permeability changes due to the deformation and growth of micro-sized rock fractures (Mahyari and Selvadurai 1998, Selvadurai *et al.* 2004, Zhang and Wang 2017). The theory of permeability change was suggested after comparing experimental data obtained from laboratory tests using rock cores (Zhou *et al.* 2006, Selvadurai and Glowacki 2008, Hu *et al.* 2010, Massart and Selvadurai 2012). Selvadurai & Glowacki (2008) found that permeability changes of surrounding groundwater can be caused by mechanical strain due to complex stress variations under the condition of isostatic compression. Massart and Selvadurai (2012) investigated the stress-induced permeability evolution in a quasi-brittle material susceptible to damage.

A linear flow condition is a basic premise to explain the correlation between hydraulic and mechanical properties. However, actual fluid flows within rock fractures become nonlinear with an increase in the flow velocity because there are rough surfaces in natural rock fractures. These nonlinear fluid flows can occur due to high pore water pressure levels exceeding 10 MPa (100 bar), especially at a nuclear waste disposal site with a depth of less than 1 km. Various studies have been conducted to understand the factors affecting a nonlinear fluid flow, such as the fracture aperture, fracture length, fracture direction, fracture connectivity, filling material, roughness, pore pressure and stress (Lucas *et al.* 2007, Ranjith 2010, Wang *et al.* 2018).

Ranjith and Viete (2011) suggested that the broadly used cubic law can be applied to the evaluation of a non-Darcian flow in the case of a low flow velocity. However, prediction differences of two orders or more can arise when the

*Corresponding author, Assistant Professor
E-mail: geotaemin@pusan.ac.kr

ISSN: 2005-307X (Print), 2092-6219 (Online)

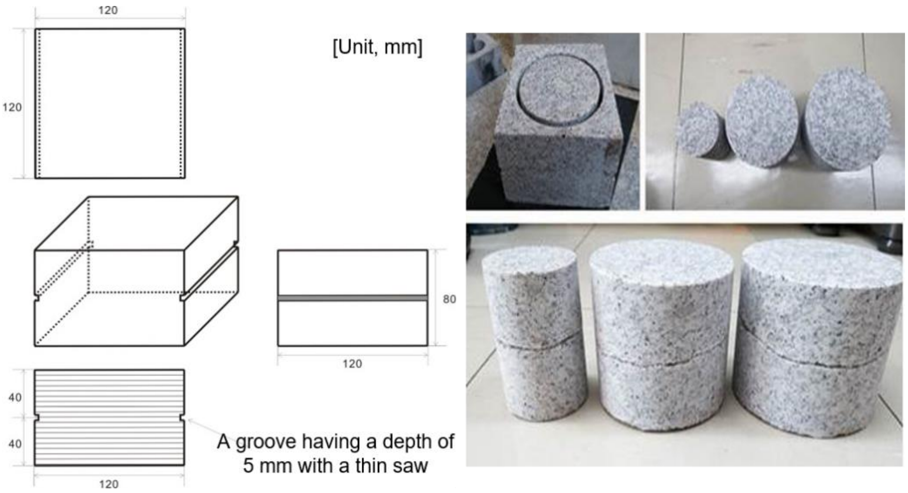

Fig. 1 Rock fracture sample (cylindrical type)

parallel plate theory is directly applied to modeling, as most natural surfaces of rock fractures are bent and irregular (Indraranta *et al.* 1999, Ranjith 2010). Ranjith (2010) demonstrated that geometry factors did not affect the fluid flow under the conditions of a low pore pressure or large aperture of rock fractures, but the conventional cubic law cannot predict the flow properties accurately due to the formation of turbulent/nonlinear flows with an increase in the pore pressure.

Subsequently, the Forchheimer and Izbash equations became widely used as nonlinear formulae when simulating flows through natural rock fractures (Forchheimer 1901, Izbash 1931). Moreover, analytical solutions were suggested to simulate a non-Darcian flow of a Newtonian fluid in fractured porous media (Barree and Conway 2004, Wu *et al.* 2011). Constant values of these equations were mostly evaluated based on a numerical analysis, but there have been few precise analyses of permeability changes according to extreme conditions (high vertical rock stress and pore water pressure).

The objective of this study is to evaluate the applicability of cubic law under a deep depth condition and suggest a hydro-mechanical correlation considering nonlinear flows through precise hydraulic tests and an effect analysis according to pressure changes (water pressure and vertical stress) and the degree of fracture roughness. To do this, we manufactured an experimental apparatus capable of generating high pore water pressure (up to 10 MPa) and vertical stress (up to 20 MPa). Moreover, we prepared a large cylindrical rock core with diameter of 10 cm using a special rock drill bit to consider the inducement of a radial permeability equation. We also measured the roughness of rock fractures and performed a quantitative analysis using three-dimensional laser scanning. Through hydraulic tests, we analyzed the rock permeability according to the vertical stress and pore water pressure with geometry (roughness). Consequently, we suggested an empirical formula of a hydro-mechanical correlation with a nonlinear property which can be applied to evaluations of changes of rock permeability levels in environments with high stress and pore water pressure, especially those at deep nuclear waste disposal repositories.

2. Materials and methods

2.1 Material and experimental setup

A rock fracture 12 cm long by 12 cm wide by 8 cm high was sampled from a massive granite outcrop in Nonsan, Korea (Fig. 1). A cylindrical rock fracture model was determined to obtain the radial permeability relationship. A fracture model with a diameter of 10 cm was manufactured using a special drill bit to consider the size effect of the rock sample. An artificial single joint was formed using uniaxial compression equipment and a metal wedge. The rectangular granite sample was vertically placed in the uniaxial compressor and the upper and lower grooves were then aligned with the pointed portion of the metal wedge and were vertically compressed and broken. As the size of the drill bit increases, precise manufacturing is difficult, and there is a strong possibility of disturbance of the rock surroundings. Unlike conventional drill operations, a precise drill operation which varied from low Revolutions per minute (rpm) to a high rpm was performed in this experiment. Three-dimensional laser scanning was performed to evaluate the quantitative roughness of the manufactured rock fracture sample.

The total set of laboratory experiments was mainly composed of two parts: a high pore water pressure controlled experiment and a high vertical stress controlled experiment. Fig. 2 shows the total experimental setup for the water permeability test in the deep underground condition (e.g., vertical stress = 20 MPa, pore water pressure = 10 MPa). It consists of the following components: a high-pressure water pump, a vertical stress controller, a high-precision flowmeter and pressure gauge, a data acquisition system, and the test section.

In this experiment, a high-pressure water pump was used to generate the high pore water pressure condition at a deep depth. This pump delivers water fluid in the form of a floating plunger piston, and it can control extremely sensitive pressure and flow rates by multicast traffic calibration. This pump can provide high pore water pressure of up to 10 MPa.

The vertical stress controller was used to reproduce

Fig. 2 Experimental setup for the permeability test with high pore water pressure and vertical stress

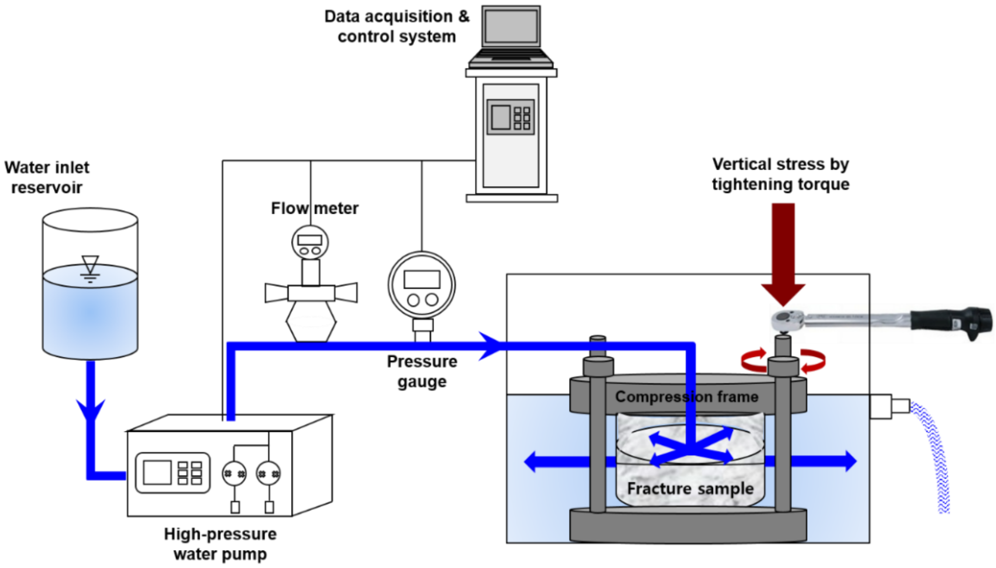

Fig. 3 Conceptual diagram and procedure for the water permeability test

vertical ground stress at a depth of less than 1 km. It can confine the rock fracture sample using clamping force (axial force) resulting from the tightening torque applied to the bolt. Vertical stress caused by the clamping force is accomplished using a torque wrench. This setup provides high vertical stress of up to 20 MPa in our experiments, and this value can be obtained by the following equation (Goldarag *et al.* 2015):

$$F_{cl} = \frac{T}{K \cdot d} \tag{1}$$

Here, F_{cl}, T and d are the clamping force, the tightening torque imposed on the bolt head and the bolt head diameter, respectively. K is the torque coefficient that depends on various parameters, in this case the geometry and friction. It has a range of 0.14 to 0.26 and is widely used with a value of 0.2 in general cases. In this study, a K value of 0.2 as suggested by Goldarag *et al.* (2015) was used to obtain the vertical stress.

Coriolis mass flowmeter with a high resolution was used to estimate accurately a very low flow rate through micro-sized rock fractures. It can estimate flow rates from 0.05-5.40 l/min and has a measurement accuracy of ± 0.1%. A digital pressure gauge was used to estimate the fluid pressure of the inlet and outlet points. It can identify pressure in a range of 0 to 15 MPa and has measurement accuracy of ± 0.025%. A multichannel data system was

Table 1 Experimental parameters of the fracture sample and test setup

Experimental Parameter	Value
Tightening torque, T (kgf·cm)	270, 540, 1080
Torque coefficient, K (-)	0.2
Bolt head diameter, d (cm)	2.4
Internal radius of the rock fracture, r_1 (cm)	0.3
External radius of the rock fracture, r_2 (cm)	5
Water viscosity, μ (kg/cm·s)	0.001

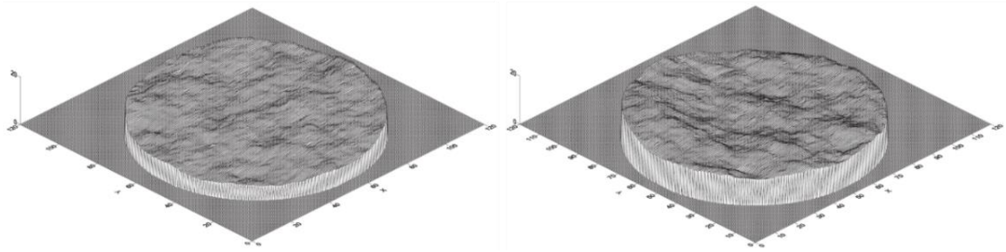

Fig. 4 Roughness measurement results (3-D profiles of the rock fracture using a laser-type displacement meter)

installed to control the experimental parameters and to acquire data. The injection condition of the pumps (injection pressure and flow rate of water fluid) was regulated using a display system. In addition, a feedback system was used to optimize and stabilize the injection conditions. Table 1 summarizes the experimental parameters of the fracture sample and experimental setup in this study.

2.2 Experimental procedures

Fig. 3 shows the conceptual diagram and procedure of the permeability test under the condition of high pore water pressure and vertical stress. First, the water injected by the high pore water pressure pump moved into the center hole of the rock fracture sample confined by the compression frame, which consisted of stainless steel. The injected water then radially flowed out through the rock and out through the rock fractures and was discharged at the outlet reservoir through an overflow nozzle. In this experiment, deaerated water was used to remove the unexpected effect of air within the water in the fluid flow. The rock sample was immersed in a water tank and the fracture surface was in a completely water-saturated condition throughout the permeability tests. This was done because water flow can show different phase flows according to the saturating condition. In addition, common rock fractures at a deep depth are in a fully saturated condition, which should be accurately reproduced in a laboratory experiment. Using equation (1), vertical stress values were determined to be 2.8, 5.6 and 11.2 MPa. At a vertical stress level above 12 MPa, the aperture of the rock fractures closed due to the vertical compression caused by the very high stress. Therefore, the vertical stress values were limited to 12 MPa or less in our experiments. Under each vertical stress condition, flow experiments were carried out according to a change in the pore water pressure. The pore water pressure imposed by this experiment was lower than the vertical stress in each case. At pore water pressure levels larger than the vertical stress, the rock fracture can be widened or broken. These exceptional cases were not considered in our experiments.

3. Results and analysis

3.1 Roughness quantitative analysis

The conventional measurement method of surface bends by a sensor contact has been widely used to evaluate roughness levels, but it has low accuracy and poor resolution of the roughness. The geometry of fracture surfaces was digitized as three-dimensional coordinate values through 3D profile measurements along the direction of the shear displacement. The joint roughness coefficient (*JRC*) was then determined using the calculated Z_2 (linear differential, the average square root) values (Tsu and Cruden 1979). The specific process of the roughness measurement in this study was as follows. First, the rock sample was placed on an experimental table parallel with the laser scan direction of a 3D laser scanner. The scan range of the displacement meter of the 3D laser scanner was determined in accordance with the experimental purposes. Many two-dimensional profile coordinates were extracted from the measured three-dimensional coordinate values. Then, Z_2 about each profile was calculated and its average value was obtained using the following equation:

$$Z_2 = \sqrt{\frac{1}{N-1}\sum_{i=1}^{N-1}\left(\frac{y_{i+1}-y_i}{\Delta x}\right)^2} \tag{2}$$

Lastly, the calculated Z_2 values were converted to *JRC* using the following equation suggested by Tse and Cruden (1979):

$$JRC = 32.20 + 32.47 log Z_2 \tag{3}$$

The *JRC* values of the rock samples were obtained through 3D profile measurements and a roughness quantitative analysis. The measurement interval was 0.5 mm. The *JRC* values used in this study were 6.2 and 10.8, which indicates moderate and strong roughness, respectively. These two cases as shown in Fig. 4 were used to evaluate permeability changes according to the pore water pressure and vertical stress in this experiment.

3.2 Influence of the vertical stress, pore water pressure and roughness on the permeability

Water permeability tests according to vertical stress and pore water pressure were conducted in rock fractures with different roughness levels. Considering cylindrical rock fractures, a modified cubic law pertaining to a radial flow was derived from the conventional cubic law of a linear flow (Selvadurai 2014), as follows:

$$b = \left[\frac{6\mu q ln\frac{r_2}{r_1}}{\pi(P_1-P_2)}\right]^{\frac{1}{3}} \tag{4}$$

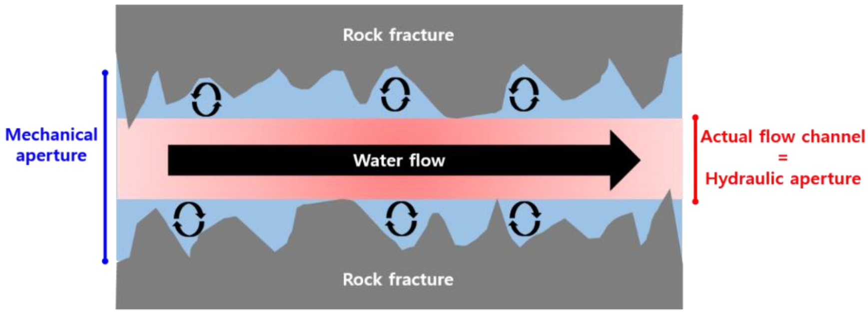

Fig. 5 Concept of the hydraulic aperture

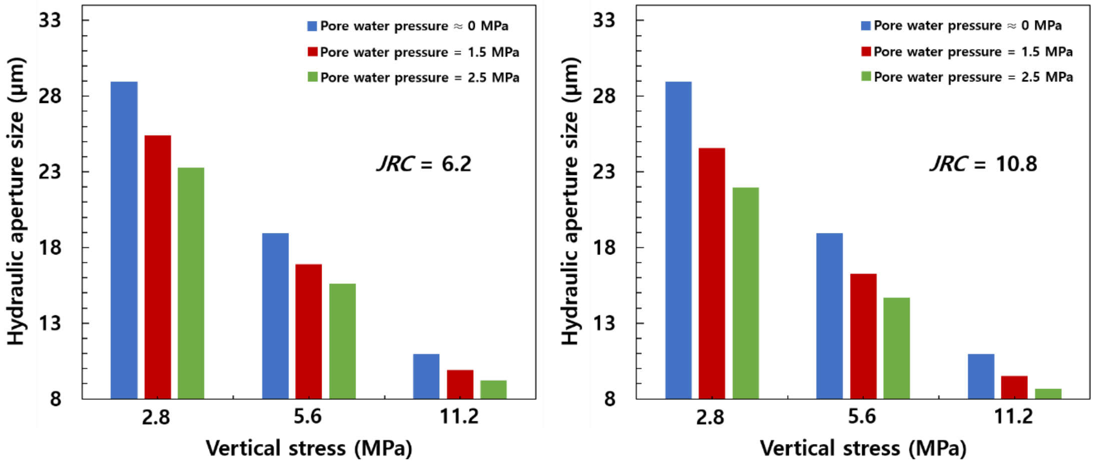

Fig. 6 Hydraulic aperture size according to the water pressure and vertical stress for *JRC* values of 6.2 and 10.8

where b is the hydraulic aperture size calculated by the cubic law, μ is the water viscosity, q is the flow rate, r_1 and r_2 are the internal and external radiuses of the cylindrical rock fracture, and P_1 and P_2 are the upstream and downstream of pore water pressures, respectively. Using this hydraulic aperture equation, the rock permeability can be calculated through the parallel plate model suggested by Zimmerman and Bodvarsson (1996), as follows:

$$k = \frac{b^2}{12} \tag{5}$$

where k is the permeability through single rock fracture.

Generally, the empty space located in a rock fracture is regarded as having a fixed geometry. This is known as a mechanical aperture, as shown in Fig. 5. In the case of a perfect parallel fracture, the mechanical aperture is completely equal to the entire flow channel. However, because there are flow disturbances (eddy flows or flow friction near the fracture wall) in natural rock fractures with rough and irregular surfaces, the mechanical aperture is different from the actual flow channel in an actual underground rock environment. The concept of a real space reflecting an actual flow channel is needed for an accurate evaluation of the groundwater permeability through rock fractures, termed the hydraulic aperture. The hydraulic aperture is universally smaller than the mechanical aperture, and it may decrease as the roughness and flow velocity increase (Roy and Singh 2015). In this study, the concept of the hydraulic aperture was used to estimate the rock permeability according to the vertical stress and pore water pressure.

Fig. 6 shows the change in the hydraulic aperture size according to the pore water pressure and vertical stress. First, in rock fractures for which JRC = 6.2, the hydraulic aperture size decreased as the vertical stress was increased from 2.8 to 11.2 MPa. At pore water pressure levels of 0, 1.5 and 2.5 MPa, the reduction ratios of the hydraulic aperture according to the vertical stress were 62.2, 61.1 and 60.3%, respectively. These reductions are due to the decrease in the mechanical aperture size caused by the vertical compression of the rock fractures. However, even under identical vertical stress conditions, there were differences in the hydraulic aperture size according to pore water pressure variations. At each vertical stress value of 2.8, 5.6 and 11.2 MPa, the reduction ratios of the hydraulic aperture according to the pore water pressure were 19.7, 17.6 and 15.6%, respectively. This reduction comes from the turbulent flow friction in natural rock fractures with rough surfaces, which intensified more as the pore water pressure increased to 2.5 MPa. In other words, the actual size of the flow channel within a rock fracture can changed by nonlinear flow behavior in even with the same geometry formed under the same vertical stress.

In case of JRC = 10.8, the overall trend of the hydraulic aperture according to the pore water pressure and vertical stress were similar to those when JRC = 6.2, as shown in the right part of Fig. 6. However, the degrees of the reduction ratio of the hydraulic aperture size according to the pore water pressure were larger than in the case of JRC = 6.2; these were 24.1, 22.6 and 20.9% at the vertical stress values of 2.8, 5.6 and 11.2 MPa, respectively. This result

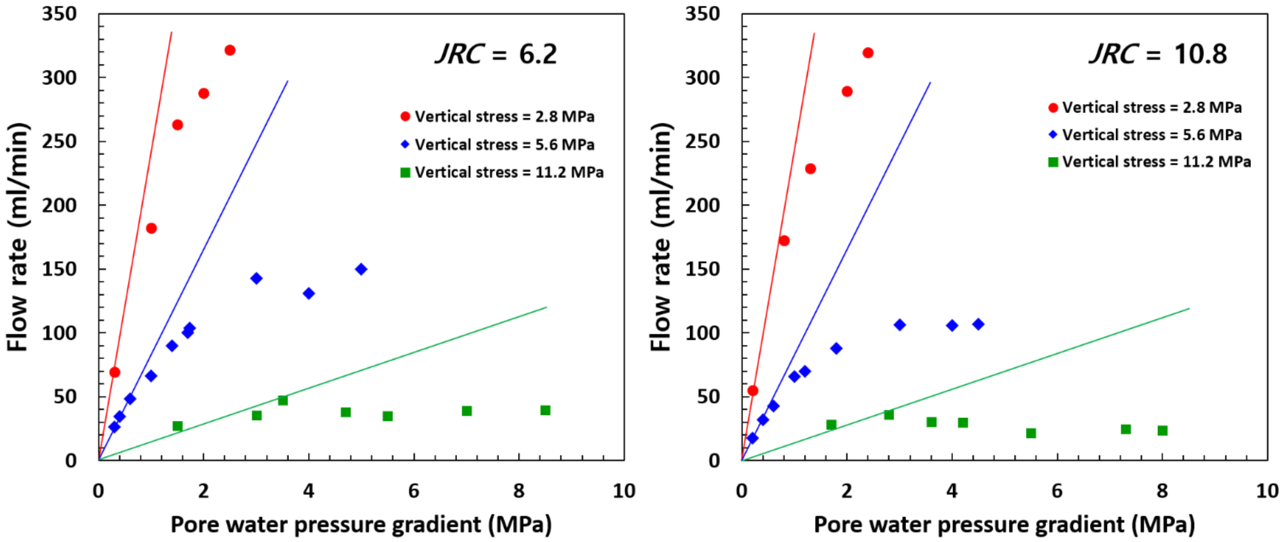

(a) Flow rate versus pore water pressure gradient

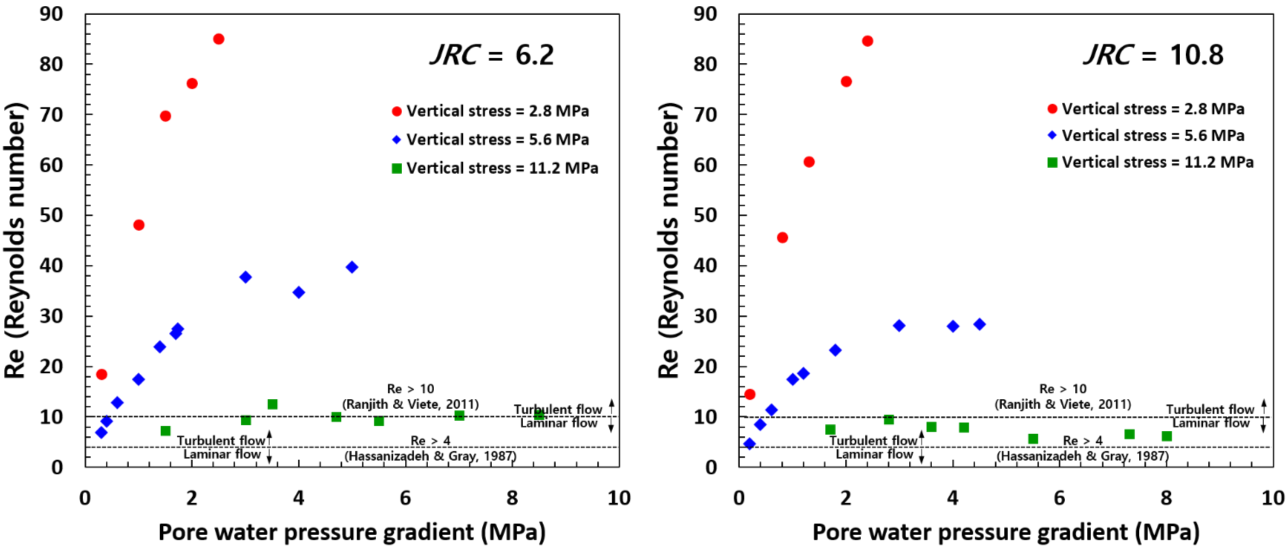

(b) Re (Reynolds number) versus pore water pressure gradient

Fig. 7 Analysis of nonlinear flow regime for all experimental cases

indicates that the roughness as well as the pore water pressure can change the hydraulic aperture.

Nonlinear flow regime was analyzed by the relationship between the outflow rate and pore water pressure gradient, as shown in Fig. 7(a). Generally, it is assumed that the linear flow through two parallel plates is governed by "Darcy's law" or "cubic law". In this case, the flow rate and pressure gradient should follow the linear trend, such as the linear solid line depicted in Fig. 7(a). However, most of the measured experimental data points deviate from the linear relationship between outflow rate and pore water pressure gradient. This consistent deviation in the flow can be result of a turbulent flow friction, which indicates that the flow through rock fracture falls into nonlinear flow regime.

Another analysis using Reynolds number was performed to clarify the flow regime, as shown in Fig. 7(b). Reynolds number, defining the flow type to be laminar (linear) or turbulent (nonlinear), is crucial for evaluating the fluid flow mechanism through rock fractures. It can be obtained by applying the measured outflow rate and sample dimension to the following relationship (Zimmerman *et al.* 2004, Ranjith and Viete 2011, Singh *et al.* 2015).

$$Re = \frac{\rho \cdot Q}{\mu \cdot W} \tag{6}$$

where ρ, Q, μ and W are the water density, outflow rate, viscosity and fracture width, respectively. Two line representing $Re > 4$ or $Re > 10$ were depicted in Fig. 7(b) as horizontal dotted lines, which serves as a criterion for determining the transition in flow from laminar to turbulent (Hassanizadeh and Gray 1987, Ranjith and Viete 2011). It can be observed that most of data points for all experimental cases fall within the range beyond Re of 10, although some data existed between Reynolds number range from 4 to 10. For this analysis, it can be confirmed that a turbulent (nonlinear) flow regime is mostly formed in fracture flow of our permeability experiments.

Fig. 8 shows the effect of the vertical stress on the permeability under different pore water pressure conditions. The permeability gradually decreased with an increase in the vertical stress. At JRC = 6.2, the reduction ratios of the

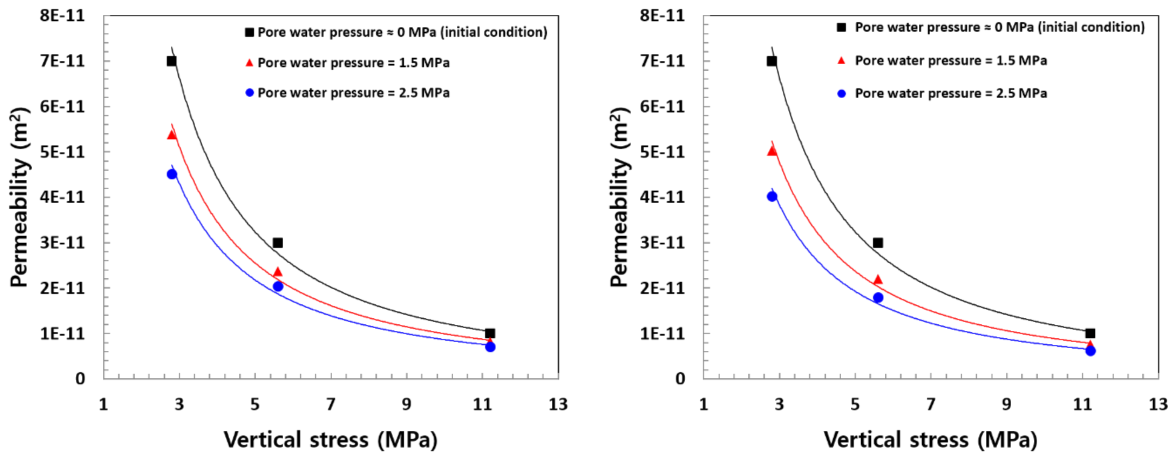

Fig. 8 Permeability changes according to the vertical stress under different pore water pressures at *JRC* values of 6.2 and 10.8

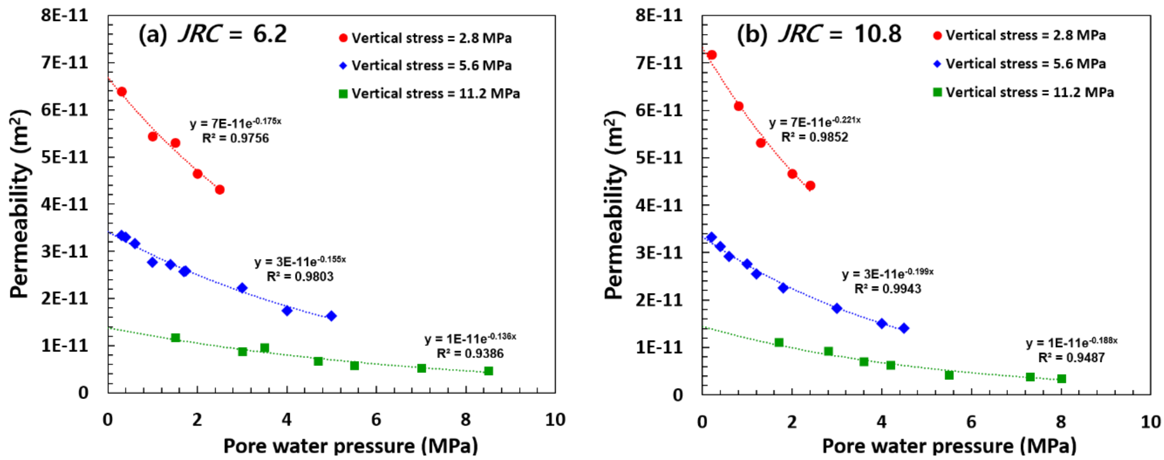

Fig. 9 Permeability changes according to the pore water pressure under different vertical stress conditions: (a) *JRC* = 6.2 and (b) *JRC* = 10.8

permeability according to the vertical stress were 85.7, 84.9 and 84.3% at pore water pressures of 0, 1.5 and 2.5 MPa, respectively. When *JRC* = 10.8, the overall trend and value of the permeability reduction were similar to those when *JRC* = 6.2. As shown in Fig. 6, this reduction of the permeability comes from the apertures of the open rock fractures, which become narrow due to space compression caused by high vertical stress. When the vertical stress exceeds 12 MPa, the rock permeability cannot be measured because the water-flowing pathway has disappeared due to the closure of the fracture aperture caused by the increased vertical stress. This means that the typical rock permeability becomes smaller with an increase in the depth under high underground pressure, referred to as vertical stress.

At *JRC* = 6.2, the reduction ratios of the permeability according to the pore water pressure were 35.4, 32.1 and 28.8% at vertical stress levels of 2.8, 5.6 and 11.2 MPa, respectively. In the case of *JRC* = 10.8, the permeability reductions according to the pore water pressure were more intensified with compared to the case of *JRC* = 6.2, showing values of 42.5, 40.1 and 37.5% at vertical stress levels of 2.8, 5.6 and 11.2 MPa, respectively. These changes are caused by flow friction due to the turbulent flow and roughness. Hence, these results imply that predictions of the permeability can differ even in rock fractures with an identical geometry at the same underground depth. In particular, permeability estimations at a deep depth may be more complicated due to the nonlinear behavior of a fast groundwater flow when an underground artificial facility such as a nuclear waste repository is developed and operated.

3.3 Modified permeability estimation under deep depth conditions

Fig. 9(a) shows the effect of the pore water pressure on changes in the fracture permeability under different vertical stress conditions when *JRC* = 6.2. Generally, a similar trend in which the water permeability decreased with an increase in the pore water pressure was observed under the vertical stress conditions of 2.8, 5.6 and 11.2 MPa. As the vertical stress was increased, the water permeability decreased. The slope of the permeability reduction under low vertical stress was steeper than that under high vertical stress. The permeability decreased exponentially as the pore water pressure was increased, and the exponent values indicating a reduction in the slope were -0.175, -0.155 and -0.136 at the vertical stress levels of 2.8, 5.6 and 11.2 MPa, respectively.

Generally, the increase of pore water pressure can

Fig. 10 Spalling of the rock sample by high pore water pressure exceeding the vertical stress

induce the expansion of fracture aperture. However, in this experimental cases, the rock fracture sample was completely confined by the steel compression frame. This equipment fixed the fracture sample under a vertical stress condition, which did not cause a change of fracture geometry such as aperture expansion. Consequently, the increase of pore water pressure intensified the flow friction due to the increase of turbulence (nonlinear flow effect), which can induce the decrease of permeability of rock fracture in this study.

The pore water pressure levels at each vertical stress were imposed up to certain values, as pore water pressure which exceeds the vertical pressure can cause a transformation of the fracture geometry, such as hydro-fracturing or fault slippage. In fact, spalling of the rock sample used in this experiments occurred when the pore water pressure exceeded the vertical stress, as shown in Fig. 10. In such cases, the intrinsic rock permeability cannot be correctly measured due to the major deformation of the fracture geometry.

Fig. 9(b) shows the water permeability according to pore water pressure changes in a rock fracture with a *JRC* value of 10.8. In this case, a rougher surface of the rock fracture was identified compared to the 6.2 *JRC* case. The rock permeability more dramatically decreased according to the pore water pressure at a rougher surface (high *JRC* value). From this result, we found that the rock permeability could be strongly affected by the fracture roughness and by the vertical stress and pore water pressure. Moreover, the conventional cubic law for evaluating the rock permeability assumes that the permeability is constant under identical pore water pressure conditions. Therefore, it cannot be applied to precise determinations of the rock permeability in cases of high vertical stress and high pore water pressure levels. For this reason, a modified equation considering the non-linear flow is needed to evaluate the permeability precisely under deep depth conditions.

The empirical correlation equation derived from the water permeability tests can be expressed as follows:

$$k_n = k_l e^{GP_w} \tag{7}$$

where k_n is the rock permeability of nonlinear flow under a deep depth condition, k_l is the rock permeability of linear flow under atmospheric pressure conditions, G is the geometric constant and P_w is the pore water pressure. Geometric constant, G, is related to the vertical stress and surface roughness of rock fracture. Values of G increase as the vertical stress increases and the fracture roughness decreases. Eq. (7) shows an exponential decrease in the rock permeability according to pore water pressure changes. In this equation, k_0 is not greatly affected by the roughness because there is little flow friction in a very slow groundwater flow. The geometric constant is affected by the fracture roughness, expressed as the *JRC* values. The average G values were -0.15 and -0.21 for the smoother surface (*JRC* = 6.2) and for the rougher surface (*JRC* = 10.8), respectively. This geometric constant will be decreased as the roughness increases, and this can be generalized by permeability tests using more rock fractures with various roughness levels.

4. Discussion

Conventionally, the permeability value is nearly identical in cases with identical effective stress levels. The effective stress is defined as the difference between the vertical stress and the pore water pressure, which is the actual confining stress acting on the fracture aperture. In other words, the rock permeability increases with a decrease in the effective stress when the pore water pressure increases. However, this experiment demonstrates that the rock permeability will decrease despite the decrease of the effective stress, and a difference of more than one order of magnitude was shown even at the same effective stress (e.g., 2 MPa, as shown in Fig. 11). The non-uniformity of the permeability of a rougher surface according to the effective stress was higher than that of a smoother surface, but the overall trend was similar in both cases. This occurs due to the occurrence of a nonlinear flow and fluid friction within the rough surfaces of rock fractures under a fast flow condition at a deep depth. The effect of the interaction between the effective stress and a nonlinear flow on the rock fracture permeability should be established to predict the accurate groundwater permeability at a deep underground facility.

Consequently, the rock permeability was affected by all

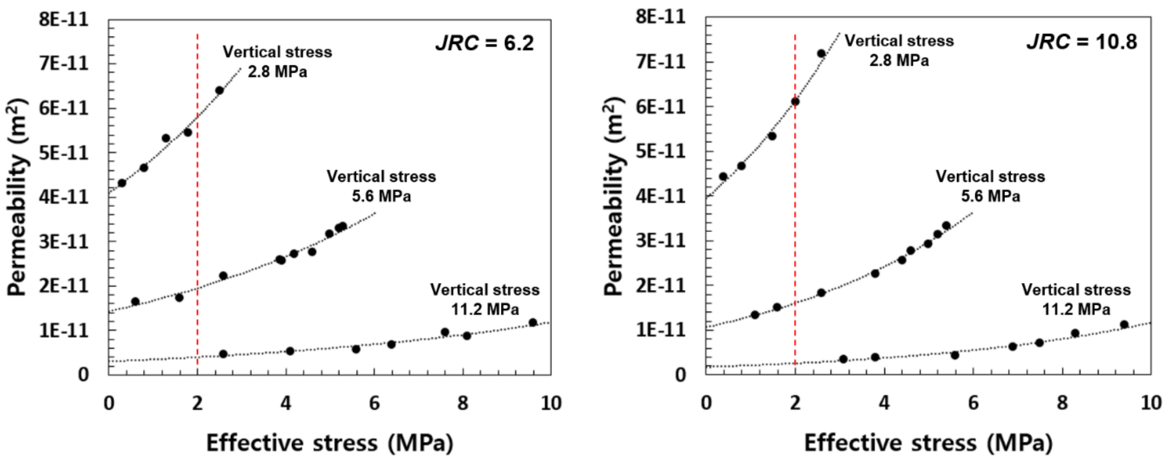

Fig. 11 Permeability versus effective stress at *JRC* values of 6.2 and 10.8

three factors of the vertical stress, pore water pressure and roughness. However, the degree of the effect of the roughness on the permeability was relatively small compared to the other two factors. The permeability can change due to the interconnection between the vertical stress and pore water pressure, which should be significantly considered during the design and operation of a nuclear waste repository located one hundred meters under fractured rock. Our understanding the variations of the rock permeability can be enhanced through the elaboration of the empirical correlation equation with much more experimental data according to various pressure conditions, surface roughness levels, and rock types.

5. Conclusions

In this study, we evaluated the application of cubic law to deep depth conditions and proposed a permeability equation considering a nonlinear fluid flow. For this purpose, we performed a quantitative analysis by 3D measurements of rock fracture roughness levels using a laser scanner. Then, we derived the radial permeability correlation equation and analyzed the influence of pressure changes on the rock permeability. Generalization of hydro-mechanical correlation equation is possible at a deep depth condition, and this is applicable to evaluations of permeability changes under high vertical stress and pore water pressure circumstances. Ultimately, the results of this study can be expected to bolster the development of evaluation and prediction improvement technology for permeability characteristics of surrounding rock masses during the construction and operation of underground facilities at deep depths. The main conclusions of our experiments are given below.

• The permeability decreases as the vertical stress increases due to the narrowing of the fracture aperture.

• The permeability exponentially decreases as the pore water pressure increases owing to the occurrence of a nonlinear flow and fluid friction through a rough fracture surface.

• Roughness strengthens the permeability change according to the vertical stress and pore water pressure.

• At a deep depth condition, a simple prediction using the existing cubic law is uncertain when seeking accurate evaluations of rock permeability levels.

• The influence of a nonlinear flow on the permeability change should be considered under high vertical stress and pore water pressure conditions.

Acknowledgments

This research was supported by the National Research Foundation of Korea (NRF) grant funded by the Korea Government (MSIT) (No. NRF-2019R1G1A1100517), and Basic Research Project of the Korea Institute of Geoscience and Mineral Resources (KIGAM) funded by the Ministry of Science and ICT of Korea.

References

Barree, R.D. and Conway, M.W. (2004), “Beyond beta factors: A complete model for Darcy Forchheimer and trans-Forchheimer flow in porous media”, *Proceedings of the SPE89325 Annual Technical Conference and Exhibition*, Houston, Texas, U.S.A., September.

Deng, D.P., Li, L. and Zhao, L.H. (2019), “Stability analysis of slopes under groundwater seepage and application of charts for optimization of drainage design”, *Geomech. Eng.*, **17**(2), 181-194. https://doi.org/10.12989/gae.2019.17.2.181.

Forchheimer, P.H. (1901), “Wasserbewegung durch boden”, *Z. Ver. Deutsch. Ing.*, **50**, 1781-1788.

Goldarag, F.E., Barzegar, S. and Babaei, A. (2015), “An experimental method for measuring the clamping force double lap simple bolted and hybrid (bolted-bonded) joints”, *T. Famena.*, **39**(3), 87-94.

Hassanizadeh, S.M. and Gray, W.G. (1987), “High velocity flow in porous media”, *Transport Porous Med.*, **2**(6), 521-531. https://doi.org/10.1007/BF00192152.

Hu, D.W., Zhu, Q.Z., Zhou, H. and Shao, J.F. (2010), “A discrete approach for anisotropic plasticity and damage in semi-brittle rocks”, *Comput. Geotech.*, **37**(5), 658-666. https://doi.org/10.1016/j.compgeo.2010.04.004.

Indraranta, B., Ranjith, P.G. and Gale, W. (1999), “Single phase water flow through rock fractures”, *Geotech. Geol. Eng.*, **17**(3-4), 211-240. https://doi.org/10.1023/A:1008922417511.

Izbash, S.V. (1931), “O filtracii V Kropnozernstom Materiale”, USSR, Lehingrad (in Russian).

Ji, S.H., Koh, Y.K. and Choi, J.W. (2012), “The state-of-the art of the borehole disposal concept for high level radioactive waste”, *J. Korean Radioactive Waste Soc*., **10**(1), 55-62. https://doi.org/10.7733/jkrws.2012.10.1.055.

Kim, J., Kim, J., Lee, J. and Yoo, H. (2018), “Prediction of transverse settlement trough considering the combined effects of excavation and groundwater depression”, *Geomech*. *Eng*., **15**(3), 851-859. https://doi.org/10.12989/gae.2018.15.3.851.

Lee, H., Oh, T.M., Park, E.S., Lee, J.W. and Kim, H.M. (2017), “Factors affecting waterproof efficiency of grouting in single rock fracture”, *Geomech*. *Eng*., **12**(5), 771-783. https://doi.org/10.12989/gae.2017.12.5.771.

Lucas, Y., Panfilov, M. and Bues, M. (2007), “High velocity flow through fractured and porous media: The role of flow non-periodicity”, *Eur*. *J*. *Mech*. *B Fluid*., **26**(2), 295-303. https://doi.org/10.1016/j.euromechflu.2006.04.005.

Mahyari, A.T. and Selvadurai, A.P.S. (1998), “Enhanced consolidation in brittle geomaterials susceptible to damage”, *Mech*. *Coh Fric*. *Mat*., **3**(3), 291-303. https://doi.org/10.1002/(SICI)1099-1484(199807)3:3<291::AID-CFM53>3.0.CO;2-K.

Massart, T.J. and Selvadurai, A.P.S. (2012), “Stress-induced permeability evolution in quasi-brittle geomaterials”, *J. Geophys*. *Res*. *Solid Earth*, **117**(B7), B07207. https://doi.org/10.1029/2012JB009251.

Najari, M. and Selvadurai, A.P.S. (2014), “Thermo-hydro-mechanical response of granite to temperature changes”, *Environ*. *Earth Sci*., **72**(1), 189-198. https://doi.org/10.1007/s12665-013-2945-3.

Nguyen, T.S. and Jing, L. (2008), “DECOVALEX-THMC Project. Task A. Influence of near field coupled THM phenomena on the performance of a spent fuel repository”, Report of Task A2, SKI Report 44, 1-100.

Ranjith, P.G. (2010), “An experimental study of single and two-phase fluid flow through fractured granite specimens”, *Environ*. *Earth Sci*., **59**(7), 1389-1395. https://doi.org/10.1007/s12665-009-0124-3.

Ranjith, P.G. and Viete, D.R. (2011), “Applicability of the ‘cubic law’ for non-Darcian fracture flow”, *J*. *Petrol*. *Sci*. *Eng*., **78**(2), 321-327. https://doi.org/10.1016/j.petrol.2011.07.015.

Roy, D.G. and Singh, T.N. (2015), “Fluid flow through rough rock fractures: Parametric study”, *Int*. *J*. *Geomech*., **16**(3), 04015067. https://doi.org/10.1061/(ASCE)GM.1943-5622.0000522.

Rutqvist, J., Freifeld, B., Min, K.B., Elsworth, D. and Tsang, Y. (2008), “Analysis of thermally induced changes in fractured rock permeability during eight years of heating and cooling at the Yucca Mountain Drift Scale Test”, *Int*. *J*. *Rock Mech*. *Min*. *Sci*., **45**(8), 1373-1389. https://doi.org/10.1016/j.ijrmms.2008.01.016.

Saberhosseini, E., Keshavarzi, R. and Ahangari, K. (2014), “A new geomechanical approach to investigate the role of in-situ stresses and pore pressure on hydraulic fracture pressure profile in vertical and horizontal oil wells”, *Geomech*. *Eng*., **7**(3), 233-246. https://doi.org/10.12989/gae.2014.7.3.233.

Selvadurai, A.P.S. (2004), “Stationary damage modelling of poroelastic contact”, *Int*. *J*. *Solids Struct*., **41**(8), 2043-2064. https://doi.org/10.1016/j.ijsolstr.2003.08.023.

Selvadurai, A.P.S. (2014), “Normal stress-induced permeability hysteresis of a fracture in a granite cylinder”, *Geofluids*, **15**(1-2), 37-47. https://doi.org/10.1111/gfl.12107.

Selvadurai, A.P.S. and Glowacki, A. (2008), “Evolution of permeability hysteresis of Indiana Limestone during isotropic compression”, *Ground Water*, **46**(1), 113-119. https://doi.org/10.1111/j.1745-6584.2007.00390.x.

Singh, K.K., Singh, D.N. and Ranjith, P.G. (2015), “Laboratory simulation of flow through single fractured granite”, *Rock Mech*. *Rock Eng*., **48**(3), 987-1000. https://doi.org/10.1007/s00603-014-0630-9.

Tse, R. and Cruden, D.M. (1979), “Estimating joint roughness coefficients”, *Int*. *J*. *Rock Mech*. *Min*. *Sci*. *Geomech*. *Abstr*., **16**(5), 303-307. https://doi.org/10.1016/0148-9062(79)90241-9.

Wang, J., Li, S.C., Li, L.P. and Gao, C.L. (2018), “Influence of fracture characters on flow distribution under different Reynold numbers”, *Geomech*. *Eng*., **14**(2), 187-193. https://doi.org/10.12989/gae.2018.14.2.187.

Wang, Z., Kwon, S., Qiao, L., Bi, L. and Yu, L. (2017), “Estimation of groundwater inflow into an underground oil storage facility in granite”, *Geomech*. *Eng*., **12**(6), 1003-1020. https://doi.org/10.12989/gae.2017.12.6.1003.

Wu, Y.S., Lai, B., Miskimins, J.L. and Fakcharoenphol, P. and Di, Y. (2011), “Analysis of multiphase non-Darcy flow in porous and fractured media”, *Transport Porous Med*., **88**(2), 205-223. https://doi.org/10.1007/s11242-011-9735-8.

Zhang, J. and Wang, X. (2017), “Permeability-increasing effects of hydraulic flushing based on flow-solid coupling”, *Geomech*. *Eng*., **13**(2), 285-300. https://doi.org/10.12989/gae.2017.13.2.285.

Zhou, J.J., Shao, J.F. and Xu, W.Y. (2006), “Coupled modeling of damage growth and permeability variation in brittle rocks”, *Mech*. *Res*. *Commun*., **33**(4), 450-459. https://doi.org/10.1016/j.mechrescom.2005.11.007.

Zimmerman, R.W. and Bodvarsson, G.S. (1996), “Hydraulic conductivity of rock fractures”, *Transport Porous Med*., **23**(1), 1-30. https://doi.org/10.1007/BF00145263.

Zimmerman, R.W., Al-Yaarubi, A.H., Pain, C.C. and Grattoni, C.A. (2004), “Nonlinear regimes of fluid flow in rock fractures”, *Int*. *J*. *Rock Mech*. *Min*. *Sci*., **41**, 1A27. https://doi.org/10.1016/j.ijrmms.2004.03.036.

GC